REPORT DOCUMENTATION PAGE

Form Approved OMB NO. 0704-0188

1. REPORT DATE (DD-MM-YYYY)	2. REPORT TYPE	3. DATES COVERED (From - To)
20-08-2012	Conference Proceeding	-

4. TITLE AND SUBTITLE	5a. CONTRACT NUMBER
A Lyapunov-based approach for Time-Coordinated 3D Path-Following of multiple Quadrotors in SO(3)	W911NF-10-1-0044
	5b. GRANT NUMBER
	5c. PROGRAM ELEMENT NUMBER
	611102

6. AUTHORS	5d. PROJECT NUMBER
Isaac Kaminer, Enric Xargay, Vladimir Dobrokhodov, Naira Hovakimyan, Venanzio Cichella, A. Pedro Aguiar, Antonio M. Pascoal	
	5e. TASK NUMBER
	5f. WORK UNIT NUMBER

7. PERFORMING ORGANIZATION NAMES AND ADDRESSES	8. PERFORMING ORGANIZATION REPORT NUMBER
University of Illinois - Urbana Grants and Contracts Office 109 Coble Hall Champaign, IL 61820 -6242	

9. SPONSORING/MONITORING AGENCY NAME(S) AND ADDRESS(ES)	10. SPONSOR/MONITOR'S ACRONYM(S)
U.S. Army Research Office P.O. Box 12211 Research Triangle Park, NC 27709-2211	ARO
	11. SPONSOR/MONITOR'S REPORT NUMBER(S)
	55839-NS.20

12. DISTRIBUTION AVAILIBILITY STATEMENT
Approved for public release; distribution is unlimited.

13. SUPPLEMENTARY NOTES
The views, opinions and/or findings contained in this report are those of the author(s) and should not contrued as an official Department of the Army position, policy or decision, unless so designated by other documentation.

14. ABSTRACT
Abstract—This paper focuses on the problem of developing control laws to solve the Time-Coordinated 3D Path-Following task for multiple Quadrotor UAVs in the presence of time-varying communication networks and spatial and temporal constraints. The objective is to enable n Quadrotors to track prede?ned

15. SUBJECT TERMS
path following, multi quadrotor, time coordinated control

16. SECURITY CLASSIFICATION OF:			17. LIMITATION OF ABSTRACT	15. NUMBER OF PAGES	19a. NAME OF RESPONSIBLE PERSON
a. REPORT	b. ABSTRACT	c. THIS PAGE			Naira Hovakimyan
UU	UU	UU	UU		19b. TELEPHONE NUMBER
					217-244-1672

Report Title

A Lyapunov-based approach for Time-Coordinated 3D Path-Following of multiple Quadrotors in SO(3)

ABSTRACT

Abstract—This paper focuses on the problem of developing control laws to solve the Time-Coordinated 3D Path-Following task for multiple Quadrotor UAVs in the presence of time-varying communication networks and spatial and temporal constraints. The objective is to enable n Quadrotors to track prede?ned spatial paths (parameterized by virtual time) while coordinating to achieve synchronization in time. One scenario is a symmetric exchange of position by four Quadrotors initially positioned in four corners of a square room. When the mission starts, every quadrotor is required to execute collision free maneuvers and arrive at the opposite corner at the same desired instant of time. In this paper, the path-following control algorithm is derived using the Special Orthogonal group theory (SO(3)), thus avoiding singularities that arise when dealing with local parameterizations of the vehicle's attitude. The coordination task is solved by adjusting the second derivative of the virtual time along the spatial paths.

A Lyapunov-based approach for Time-Coordinated 3D Path-Following of multiple Quadrotors in $\mathsf{SO}(3)$

Venanzio Cichella [†], Isaac Kaminer [†], Enric Xargay [‡], Vladimir Dobrokhodov [†],
Naira Hovakimyan [‡], A. Pedro Aguiar [§] and António M. Pascoal [§]

[†] *Naval Postgraduate School, Monterey, CA 93943.*
[‡] *University of Illinois at Urbana-Champaign, Urbana, IL 61801.*
[§] *Instituto Superior Técnico, Lisbon, 1049 Portugal*

Abstract—This paper focuses on the problem of developing control laws to solve the *Time-Coordinated 3D Path-Following* task for multiple Quadrotor UAVs in the presence of time-varying communication networks and spatial and temporal constraints. The objective is to enable n Quadrotors to track predefined spatial paths (parameterized by *virtual time*) while coordinating to achieve synchronization in time. One scenario is a symmetric exchange of position by four Quadrotors initially positioned in four corners of a square room. When the mission starts, every quadrotor is required to execute collision free maneuvers and arrive at the opposite corner at the same desired instant of time. In this paper, the path-following control algorithm is derived using the Special Orthogonal group theory ($\mathsf{SO}(3)$), thus avoiding singularities that arise when dealing with local parameterizations of the vehicle's attitude. The coordination task is solved by adjusting the second derivative of the virtual time along the spatial paths.

I. INTRODUCTION

Avoiding harm's ways requires the employment of intelligent autonomous vehicles. Combined with recent advances in miniature technology brings a global spotlight on the development of Unmanned Aerial Vehicles (UAVs). Currently, the use of UAVs plays a crucial role in preventing exposure of human beings to uncertain and hostile environments, therefore avoiding any danger to lives of operators. For instance, after being struck by the biggest recorded earthquake and a devastating tsunami, Japan has been fighting a potential nuclear catastrophe deploying UAVs in situations where the presence of human operators was hazardous.

From a design point of view, and with a slight abuse of terminology, UAVs can be classified in two main categories: fixed-wings and rotary-wings. Compared to the fixed-wings, that cannot freely move in any direction (rotate) or hold a constant position, rotorcrafts can be deployed in a much wider variety of scenarios. Among the rotary-wings aircraft, Quadrotors play an important role in research areas as prototypes for real life missions, including monitoring and exploration of small area.

A Quadrotor consists of four blades, whose motion control is achieved by adjusting the rotation rate of one or more rotor discs. Control of Quadrotors is quite challenging and

has been addressed in many recent publications. To mention a few, in [1] and [2] a stabilization and control algorithm is developed using Lyapunov stability theory. In [3] and [4] PD^2 and PID architectures are compared with LQR based control theory. Backstepping control is proposed in [5], while in [6] and [7] a visual based feedback control law is presented using camera measurements for pose estimation. Fuzzy logic control techniques are proposed in [8]. Intelligent control, based on neural networks, is introduced in [9] to achieve vertical take off and landing. Finally, integral sliding mode and reinforcement learning control are presented in [10] as solutions for accommodating the nonlinear disturbances for outdoor altitude control. The PF (path following) control law presented in this paper is motivated by [11], where a Lyapunov based control is formulated using the Special Orthogonal group ($\mathsf{SO}(3)$) theory, leading to a simple and singularity free solution for the trajectory tracking problem. A similar idea has already been adopted by the authors in [12], where a solution for the 3D PF problem for fixed-wings UAVs was presented. Furthermore, motivated by more challenging scenarios, the same algorithm was employed in [13], where multiple fixed-wings UAVs were asked to coordinate while following their desired paths.

Cooperation between multiple unmanned vehicles has received significant attention of control community in recent years. Relevant work includes spacecraft formation flying [14], UAV control [15], [16], coordinated control of land robots [17], and control of multiple autonomous underwater vehicles [18], [19]. However, much work remains to be done to overcome numerous critical constraints. For example one of the crucial problems is the presence of time-varying communication networks that arise due to temporary loss of communication links and switching communication topologies [20], [21].

Motivated by these challenges, the objective of the paper is to *enable a set of Quadrotor UAVs to converge and follow a set of desired paths under stringent temporal constraints*. A typical example is captured in Figure 1, where a set of vehicles, starting from random initial positions, must arrive at their final positions at the same time t_f, and hold a specified formation. The solution proposed consists of two basic steps: first, a PF control law is designed to drive each vehicle on a predefined spatial path $x_{d,i}(\gamma)$. To achieve the objective,
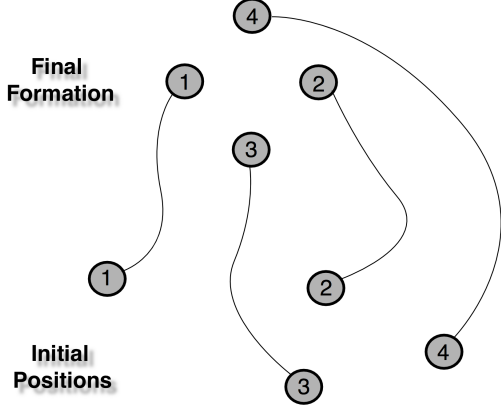
Final Formation

Initial Positions

Fig. 1: A typical example of a fleet of UAVs coordinating along predefined paths

the PF algorithm produces angular rates and thrust command, which are sent to an onboard Autopilot (AP); second, synchronization is achieved by adjusting the accelerations, thus obtaining, indirectly, vehicle coordination. Figure 2 captures the key concept described above.

This paper is organized as follows. Section II defines the PF problem for a single Quadrotor UAV. Section III formulates the Time-Coordination (TC) problem for a fleet of vehicles. In Section IV the two problems developed in the previous Sections are combined, giving a definition of Time-Coordinated 3D Path-Following (TCPF). Section V addresses the stability and convergence properties of the TCPF problem. Section VI presents simulation results. Finally, Section VII summarizes the key results and presents the main conclusions.

II. 3D PATH-FOLLOWING

A. Problem Formulation

The basic idea pursued in this paper is to reparameterize an existing trajectory tracking controller as a path following controller. In this paper we adopt with minor changes the trajectory tracking controller developed in [11] . Thus, for completeness of presentation, we follow the notation introduced in [11] and next briefly summarize the trajectory tracking controller development reported there and rewrite it as a path following controller.

Let $\mathcal{I} = [\vec{e}_1, \vec{e}_2, \vec{e}_3]^\top$ and $\mathcal{B}_i = [\vec{b}_{1,i}, \vec{b}_{2,i}, \vec{b}_{3,i}]^\top$ be two coordinate frames representing the inertial frame and the body frame attached to the i-th Quadrotor. Let also $x_{d,i}(\gamma_i)$ be a desired path parameterized by γ_i. The choice of the parameter γ_i is discussed later.

Let the motion of the Quadrotor be governed by

$$\begin{cases} \dot{x}_i = v_i \\ m\dot{v}_i = f_i\vec{b}_{3,i} - mg\vec{e}_3 \\ \dot{R}_i = R_i S(\omega_i), \end{cases} \tag{1}$$

where $x_i(t)$ and $v_i(t)$ are the position and velocity of the i-th Quadrotor, m is its mass (with no loss of generality,

it is assumed that all the Quadrotors have the same mass), $f_i(t)$ is the total thrust of the four propellers, $R_i = R_{B_i}^I$ the rotation matrix from the body frame to the inertial frame, and $\omega_i = [p_i(t), q_i(t), r_i(t)]$ the angular velocity of the vehicle expressed in $\mathcal{B}_i$. Then, we can define the position error vector $e_{x,i} \in \mathbb{R}^3$ as

$$e_{x,i}(t) = x_{d,i}(\gamma_i) - x_i(t) \tag{2}$$

and the velocity error vector $e_{v,i} \in \mathbb{R}^3$ as

$$e_{v,i}(t) = \frac{\partial x_{d,i}(\gamma_i)}{\partial \gamma_i} - \dot{x}_i(t). \tag{3}$$

Assume that the position error and the desired velocity and acceleration are bounded, that is:

$$||e_{x,i}|| \leq e_{x,i\,\max} \tag{4}$$

$$\left|\left|\frac{\partial x_{d,}}{\partial \gamma_i}\right|\right| \leq b_{1,i} \tag{5}$$

$$\left|\left|\frac{\partial^2 x_{d,i}}{\partial \gamma_i^2}\right|\right| \leq b_{2,i} \tag{6}$$

for some $b_{1,i}, b_{2,i} > 0$, and let

$$e_{x\,\max} = \sum_{i=1}^n e_{x,i\,\max},$$

$$b_1 = \sum_{i=0}^n b_{1,i}, \quad b_2 = \sum_{i=0}^n b_{2,i}.$$

Following [11], we now introduce an auxiliary frame $\mathcal{D}_i$, which is used to shape the approach to the path as a function of the error components $e_{x,i}$ and $e_{v,i}$. Let the rotation matrix from the frame $\mathcal{D}_i$ to the inertial frame $\mathcal{I}$ be

$$R_{D_i}^I = R_{c,i} = [\vec{b}_{1D,i}, \vec{b}_{3D,i} \times \vec{b}_{1D,i}, \vec{b}_{3D,i}]$$

where

$$\vec{b}_{3D,i} = \frac{k_x e_{x,i} + k_v e_{v,i} + mg\vec{e}_3 + m\frac{\partial^2 x_{d,i}}{\partial \gamma_i^2}}{||k_x e_{x,i} + k_v e_{v,i} + mg\vec{e}_3 + m\frac{\partial^2 x_{d,i}}{\partial \gamma_i^2}||} \tag{7}$$

and $\vec{b}_{1D,i}$ is chosen in order to be orthonormal to $\vec{b}_{3D,i}$. The vector $\vec{b}_{3D,i}$ defines the desired orientation of the z-axis of the Quadrotor i ($\vec{b}_{3,i}$).

Assume

$$||k_x e_{x,i} + k_v e_{v,i} + mg\vec{e}_3 + m\frac{\partial^2 x_{d,i}}{\partial \gamma_i^2}|| \neq 0, \tag{8}$$

and

$$||mg\vec{e}_3 + m\frac{\partial^2 x_{d,i}}{\partial \gamma_i^2}|| < B_i, \tag{9}$$

for any $B_i \geq 0$.

Let $\tilde{R}_i$ be the rotation matrix from $\mathcal{B}_i$ to $\mathcal{D}_i$, that is

$$\tilde{R}_i = R_{B_i}^{D,i} = R_{c,i}^\top R_i.$$

Then,

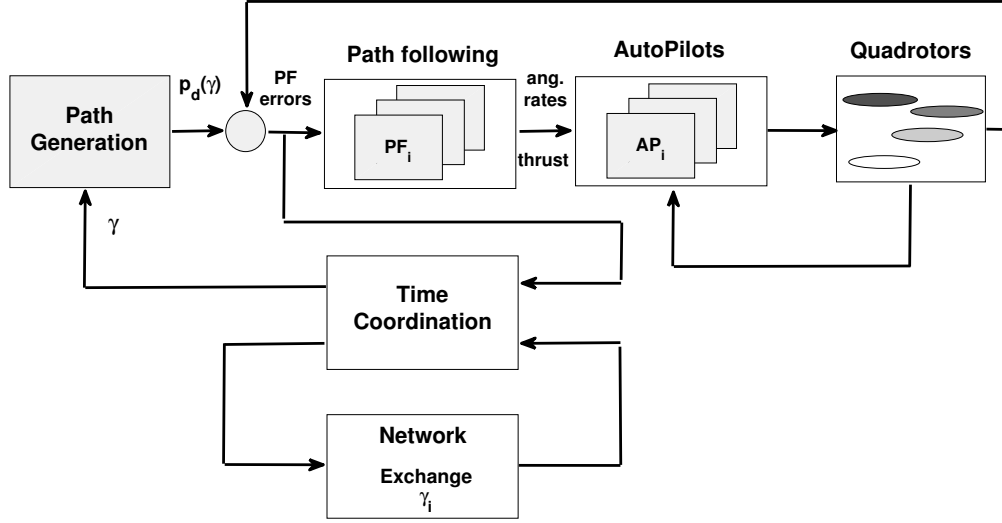$$\dot{\tilde{R}}_i = \tilde{R}_i S(\tilde{\omega}_i)$$

Fig. 2: TCPF Control Scheme

where

$$\tilde{\omega}_i = \omega_{B_i D_i}^{B_i} = \begin{bmatrix} p_i \\ q_i \\ r_i \end{bmatrix} - \tilde{R}_i^\top \omega_{D_i I}^{D_i}, \qquad (10)$$

and

$$S(\omega_{D_i I}^{D,i}) = R_{c,i}^\top \dot{R}_{c,i}.$$

Note that, if we have $\tilde{R}_i = I$, the frame $\mathcal{B}_i$ overlaps the desired frame $\mathcal{D}_i$.

Then, the objective of the controller developed is to drive the position error $e_{x,i}$ and the velocity error $e_{v,i}$ to zero, and the rotation matrix $\tilde{R}_i$ to the identity.

Consider the real-valued function on SO(3):

$$\Psi(\tilde{R}_i) = \frac{1}{2} tr(I - \tilde{R}_i), \qquad (11)$$

and its time derivative

$$\dot{\Psi}(\tilde{R}_i) = -\frac{1}{2} tr(\tilde{R}_i S(\tilde{\omega}_i)).$$

Finally, let the attitude error vector be

$$e_{\tilde{R},i} = \sqrt{\Psi(\tilde{R}_i)(2 - \Psi(\tilde{R}_i))} = \frac{1}{2} vec(\tilde{R}_i - \tilde{R}_i^\top). \qquad (12)$$

Using properties of the SO(3) group [22], we get:

$$\dot{\Psi}(\tilde{R}_i) = \frac{1}{2} e_{\tilde{R},i} \cdot \tilde{\omega}_i. \qquad (13)$$

Therefore, the dynamic of the PF errors can be summarized in the following system of equations:

$$\begin{cases} \dot{e}_{x,i} = \frac{\partial x_{d,i}}{\partial \gamma_i} \dot{\gamma}_i - \dot{x}_i \\ m\dot{e}_{v,i} = m\frac{\partial^2 x_{d,i}}{\partial \gamma_i^2} \dot{\gamma}_i - f_i \vec{b}_{3,i} + mg\vec{e}_3 \\ \dot{\Psi}(\tilde{R}_i) = \frac{1}{2} e_{\tilde{R},i} \cdot \tilde{\omega}_i. \end{cases} \qquad (14)$$

Using the above notation, we now define the PF for a single vehicle.

Definition 1: **Path-Following Problem (PF):** For a given i-th Quadrotor UAV, and for a given path $x_{d,i}(\gamma)$, design feedback control laws for the total thrust $f_i(t)$, the roll rate $p_i(t)$, pitch rate $q_i(t)$ and yaw rate $r_i(t)$ such that the generalized PF error vector $x_{PF,i} = [e_{x,i}, e_{v,i}, e_{\tilde{R},i}]$, with the dynamic described in (14), converges to a neighborhood of the origin, for any physically feasible temporal speed assignment.

B. Quadrotor with autopilot

A typical Quadrotor is equipped with an onboard AP, that stabilizes the body and tracks the thrust and angular velocities reference commands. Therefore, it is necessary to take into account possible limits on the performance of the AP inner-loop. Thus, we assume that :

$$|p_{c,i}(t) - p_i(t)| \leq \delta_{p,i} \qquad (15)$$

$$|q_{c,i}(t) - q_i(t)| \leq \delta_{q,i} \qquad (16)$$

$$|r_{c,i}(t) - r_i(t)| \leq \delta_{r,i} \qquad (17)$$

$$|f_{c,i}(t) - f_i(t)| \leq \delta_{f,i} \qquad (18)$$

where $p_{c,i}(t)$, $q_{c,i}(t)$, $r_{c,i}(t)$, $f_{c,i}(t)$ are the commanded inputs from the controller to the AP, $p_i(t)$, $q_i(t)$, $r_i(t)$, $f_i(t)$ are the actual commanded values from the inner loop architecture to the vehicle, and $\delta_{p,i}, \delta_{q,i}, \delta_{r,i}, \delta_{f,i}$ are the bounds which characterize the tracking performance of the AP. Finally, let be

$$\delta_p \triangleq \sum_{i=1}^n \delta_{p,i}, \quad \delta_q \triangleq \sum_{i=1}^n \delta_{q,i},$$

$$\delta_r \triangleq \sum_{i=1}^n \delta_{r,i}, \quad \delta_f \triangleq \sum_{i=1}^n \delta_{f,i}.$$

III. TIME-COORDINATION OF A FLEET OF QUADROTOR UAVS: PROBLEM FORMULATION

We now address the problem of the TC of a fleet of n Quadrotor UAVs.

As described in the Section II, the desired path of every vehicle is parameterized by some variable γ_i, with $i = 1, ..., n$. The choice of the parameter γ_i is such that, if $\gamma_i - \gamma_j = 0 \, \forall i, j, \quad i \neq j$ and $\dot{\gamma}_i = 1$ at some final time t_f then all the vehicles arived at their destinations at the same time.

To achieve time synchronization the parameters γ_i have to be exchanged among the Quadrotors over a communication network. Using tools from graph theory we model the information exchanged over the time-varying network as well as the constraints imposed by the communication topology. We start by assuming that the i-th UAV communicates only with a neighboring set of vehicles, denoted by $\mathcal{G}_i$. We also assume that the communication between two UAVs is bidirectional with no delays. The reader is referred to [23] for key concepts and details on algebraic graph theory.

Following the notation used in [13], we now let $L(t) \in \mathbb{R}^{n \times n}$ be the Laplacian of the graph $\Gamma(t)$. Let $Q \in \mathbb{R}^{(n-1) \times n}$ be a matrix such that $Q\mathbf{1}_n = 0$, $QQ^\top = I_{n-1}$ and $\bar{L}(t) = QL(t)Q^\top$, where $\bar{L} \in \mathbb{R}^{(n-1) \times (n-1)}$ with the spectrum equal to the spectrum of $L(t)$ without the eigenvalue $\lambda_1 = 0$. Finally, we let $\bar{L}(t)$ satisfy the persistency of excitation (PE) assumption:

$$\int_t^{t+T} \bar{L}(\tau)d\tau \geq \mu I_{n-1}. \tag{19}$$

Given the above notation, we now let

$$\xi(t) = Q\gamma(t) \tag{20}$$

where $\xi(t) = [\xi_1(t), \xi_2(t), ..., \xi_{n-1}(t)] \in \mathbb{R}^{n-1}$ and $\gamma(t) = [\gamma_1(t), \gamma_2(t), ..., \gamma_n(t)] \in \mathbb{R}^n$. From the definition of Q, if $\xi(t) = \mathbf{0}^n$, then $\gamma_i - \gamma_j = 0 \quad \forall i, j = 1, ..., n$.

Let also

$$z(t) = \dot{\gamma}(t) - 1, \tag{21}$$

where $z(t) = [z_1(t), z_2(t), ..., z_n(t)] \in \mathbb{R}^n$. Note that if $z_i = 0$ then $\gamma_i = t$.

With the above notation, the coordination problem can now be defined.

Definition 2: **Time Coordination Problem (TC):** Given a set of n 3D desired trajectories $x_{d,i}(\gamma_i)$, design feedback control law for $\ddot{\gamma}_i$ such that the vectors ξ and z defined in (20) and (21), converge exponentially to a neighborhood of the origin $\forall i = 1, ..., n$.

IV. TIME-COORDINATED 3D PATH-FOLLOWING: PROBLEM FORMULATION

In the previous sections we formulated the PF problem for a single vehicle, and the TC problem for a fleet of n Quadrotor UAVs. In this section we combine these two by defining the

TCPF problem. Consider the dynamic of the PF error variables in (14). Using the variable z defined in (21), we get

$$\begin{cases} \dot{e}_{x,i} = \frac{\partial x_{d,i}}{\partial \gamma_i} z_i + e_{v,i} \\ m\dot{e}_{v,i} = m\frac{\partial^2 x_{d,i}}{\partial \gamma_i^2} z_i + m\frac{\partial^2 x_{d,i}}{\partial \gamma_i^2} - f\vec{b}_{3,i} + mg\vec{e}_3 \\ \dot{\Psi}(\tilde{R}_i) = \frac{1}{2}e_{\tilde{R},i} \cdot \tilde{\omega}_i. \end{cases} \tag{22}$$

$\forall i = 1, ..., n$.

Let e_x, e_v, $e_{\tilde{R}}$ and $\Psi(\tilde{R})$ be

$$e_x = [e_{x,1}^\top, e_{x,2}^\top, ..., e_{x,n}^\top]^\top \in \mathbb{R}^{3n \times 1}, \tag{23}$$

$$e_v = [e_{v,1}^\top, e_{v,2}^\top, ..., e_{v,n}^\top]^\top \in \mathbb{R}^{3n \times 1}, \tag{24}$$

$$e_{\tilde{R}} = [e_{\tilde{R},1}^\top, e_{\tilde{R},2}^\top, ..., e_{\tilde{R},n}^\top]^\top \in \mathbb{R}^{3n \times 1}, \tag{25}$$

and

$$\Psi(\tilde{R}) = \sum_{i=1}^n \Psi(\tilde{R}_i) \in \mathbb{R}, \tag{26}$$

and let $x_{PF} = [e_x^\top, e_v^\top, e_{\tilde{R}}^\top]^\top$. Recall also the TC error variables defined in (20) and (21). Then, the main objective of this paper can be stated as follows:

Definition 3: **Time Coordinated 3D Path Following Problem (TCPF):** Given a fleet of n UAVs, a communication network satisfying (19) and a set of n 3D desired trajectories $x_{d,i}(\gamma_i)$, design feedback control laws for the total thrust $f_i(t)$ and for roll rate $p_i(t)$, pitch rate $q_i(t)$ and yaw rate $r_i(t)$ such that the PF errors, with the dynamic described in (22), converge to a neighborhood of the origin $\forall i = 1, ..., n$. Also, design a feedback control law for $\ddot{\gamma}_i$ such that the TC errors defined in (20) and (21) converge to zero.

V. TIME-COORDINATED 3D PATH-FOLLOWING: MAIN RESULT

First, let the total thrust of the i-th vehicle be governed by

$$f_i = \left(k_x e_{x,i} + k_v e_{v,i} + mge_3 + m\frac{\partial^2 x_{d,i}}{\partial \gamma_i^2}\right)^\top \vec{b}_{3,i}. \tag{27}$$

In addition, let the angular rates of the i-th quadrotor be

$$\begin{bmatrix} p_i \\ q_i \\ r_i \end{bmatrix} = \tilde{R}_i^\top \omega_{D_i I}^{D_i} - 2k_{\tilde{R}} e_{\tilde{R},i}. \tag{28}$$

Finally, let

$$\ddot{\gamma} = \dot{z} = -bz - aL\gamma - \underbrace{\begin{bmatrix} \alpha_{1,1}^\top e_{x,1} \\ \alpha_{1,2}^\top e_{x,2} \\ ... \\ \alpha_{1,n}^\top e_{x,n} \end{bmatrix} - \begin{bmatrix} \alpha_{2,1}^\top e_{v,1} \\ \alpha_{2,2}^\top e_{v,2} \\ ... \\ \alpha_{2,n}^\top e_{v,n} \end{bmatrix}}_{\triangleq -\bar{\alpha}(e_x, e_v)}, \tag{29}$$

where

$$\alpha_{1,i} = \left(k_x \frac{\partial x_{di}}{\partial \gamma_i} + c_1 \frac{\partial^2 x_{di}}{\partial \gamma_i^2}\right)$$

and

$$\alpha_{2,i} = \left(c_1 \frac{\partial x_{di}}{\partial \gamma_i} + m_i \frac{\partial^2 x_{di}}{\partial \gamma_i^2}\right)$$

Remark 1: Note, we modified the controller used in [11] in two important ways. First, we reparametrized it as path following controller and second we modified it to use angular rates and thrust as control inputs to be followed by an existing inner-loop autopilot. In turn, this compels us to consider the underlying performance limitations due to the constrains of the inner-loop controller.

Then, the Lemma below states one of the main results of this paper:

Lemma 1: **TCPF with ideal inner-loop tracking performance:** Let the total thrust and the angular velocities of each quadrotor be governed by (27) and (28). Let also $\ddot{\gamma}_i$ be driven by (29). Then, there exist k_x, k_v, $k_{\tilde{R}}$, c_1, a and b such that the error vector

$$x = [e_x^\top, e_v^\top, e_{\tilde{R}}^\top, \xi^\top, z^\top]^\top \tag{30}$$

converges exponentially to *zero* with rate of convergence

$$\lambda \triangleq \min(\lambda_{PF}, \lambda_{TC}), \tag{31}$$

for any

$$\lambda_{PF} > 0 \tag{32}$$

and with

$$\lambda_{TC} < \frac{\mu}{T(1+n^2 T)^2} \tag{33}$$

and corresponding domain of attraction

$$\Omega_c \triangleq \left\{ (e_x, e_{\tilde{R}}) \mid \Psi(\tilde{R}) \leq c^2 < 1, \|e_x\| \leq e_{x\,\max} \right\}. \tag{34}$$

A proof of this result is omitted due to the page limitation; however its brief outline is given in Appendix A.

As our last step, we consider the case of non perfect inner-loop discussed in Section II-B. The main result of our paper follows.

Lemma 2: **TCPF with non perfect inner-loop tracking performance:** Let the total thrust and the angular velocities of each quadrotor be governed by (27) and (28). Let also $\ddot{\gamma}$ be driven by (29). Let θ be a positive constant such that

$$0 < \theta < \lambda, \tag{35}$$

where λ was defined in (31). Let also the performance bounds defined in Section II-B, satisfy

$$\gamma_f < \frac{e_{x\,\max} k_x m \theta}{2c_1}, \tag{36}$$

and

$$\gamma_\omega \triangleq \sqrt{\gamma_p^2 + \gamma_q^2 + \gamma_r^2} < \frac{c\theta}{2-c^2}. \tag{37}$$

Then, there exist k_x, k_v, $k_{\tilde{R}}$, c_1, a and b such that, for any initial state $x(0) \in \Omega_c$ there is a time $T_b \geq 0$ such that the bound in (38) holds $\forall\ 0 \leq t < T_b$, and the bound in (39) holds $\forall\ t \geq T_b$.

The outline of the proof is given in Appendix B.

Remark 2: Note, as $\gamma_p, \gamma_q, \gamma_r$ and γ_f go to zero, we recover ideal performance shown in Lemma 1

VI. SIMULATION RESULTS

In this Section, simulation results are presented. The scenario involves four vehicles. The UAVs are asked to follow four intersecting paths. The geometry of the paths, and the constant desired speed profiles, are chosen to ensure collision avoidance. Figure 3 illustrates the above scenario. UAV$_A$ starts its mission far away from the desired initial position. This initial PF error implies an initial divergence of $\dot{\gamma}_A$ from the desired value. However, as shown in Figure 4 and 5, despite this initial error, the control algorithm ensures the convergence to the origin of the coordination states and collision free exchange of positions.

Finally, Figure 6 illustrates the performance of the PF control algorithm.

VII. CONCLUSION

This paper considered the problem of steering a fleet of Quadrotor UAVs along the predefined spatial paths, while coordinating with each other, according to the mission requirements. Cooperative control is achieved in the presence of time-varying communication networks, and stringent temporal constraints. The constraints include collision-free maneuver and simultaneous arrival at the desired locations. The PF problem is solved using the SO(3) theory, which avoids the singularities that arise when using local parametrization of the vehicle's attitude. Angular velocities and total thrust are used to drive the Quadrotors to the desired positions. Non-ideal inner-loop tracking performance is also considered. Coordination between the UAVs is achieved by adjusting the acceleration along the desired trajectories. The exponential convergence of the TCPF errors is guaranteed and demonstrated using Lyapunov theory.

REFERENCES

[1] S. Bouabdallah, P. P. Murrieri, and R. Siegwart, "Design and control of an indoor micro quadrotor," in *Proc. of The International Conference on Robotics and Automation (ICRA)*, 2004.

[2] A. Dzul, P. Castillo, and R. Lozano, "Real-time stabilization and tracking of a four rotor mini rotorcraft," in *IEEE Transaction on Control System Technology*, vol. 12(4), 2004, pp. 510–516.

[3] A. Tayebi and S. McGilvray, "Attitude stabilization of a vtol quadrotor aircraft," in *IEEE Transaction on Control System Technology*, vol. 14(3), May 2006, pp. 562–571.

[4] S. Bouabdallah, A. Noth, and R. Siegwart, "Pid vs lqr control techniques applied to an indoor micro quadrotor," in *International Conference on Intelligent Robots and Systems*, 2004.

[5] N. Guenard, T. Hamel, and V. Moreau, "Dynamic modeling and intuitive control strategy for an x4-flyer," in *International Conference on Robotics and Automation (ICRA)*, 2005, pp. 141–146.

[6] E. Altug, J. P. Ostrowski, and R. Mahony, "Control of a quadrotor helicopter using visual feedback," in *Proc. of the 2002 IEEE International Conference on Robotics and Automation (ICRA)*, 2002, pp. 72–77.

[7] N. Guenard, T. Hamel, and R. Mahony, "A practical visual servo control for an unmanned aerial vehicle," in *IEEE Transaction on Robotics*, vol. 24(2), 2008, pp. 331–340.

[8] C. Coza and C. J. B. Macnab, "A new robust adaptive-fuzzy control method applied to quadrotor helicopter stabilization," in *Annual meeting of the North American Fuzzy Information Processing Society*, 2006, pp. 454–458.

[9] M. Tarbouchi, J. Dunfied, and G. Labonte, "Neural network based control of a four rotor helicopter," in *International Conference on Industrial Technology*, 2004, pp. 1543–1548.

$$\frac{k_x}{2}||e_x(t)||^2 + \frac{m}{2}||e_v(t)||^2 + \Psi(\tilde{R}(t)) + c_1(e_v(t)^\top e_x(t)) + \frac{b^2\bar{c}_3}{2n}||\xi(t)||^2 + \frac{b\bar{c}_3}{n}\xi(t)^\top z(t) + \frac{1}{2}\left(\frac{\bar{c}_3}{n} + 1\right)||z(t)||^2 \leq$$
$$\left(\frac{k_x}{2}||e_x(0)||^2 + \frac{m}{2}||e_v(0)||^2 + \Psi(\tilde{R}(0)) + c_1(e_v(0)^\top e_x(0)) + \right. \tag{38}$$
$$\left. + \frac{b^2\bar{c}_4}{2\gamma_\lambda}||\xi(0)||^2 + \frac{b\bar{c}_4}{\gamma_\lambda}\xi(0)^\top z(0) + \frac{1}{2}\left(\frac{\bar{c}_4}{\gamma_\lambda} + 1\right)||z(0)||^2\right)e^{-(\lambda-\theta)t}$$

$$||e_x|| \leq \frac{2c_1\delta_f}{k_x m\theta(1-\epsilon_x)}\,,\ ||e_v|| \leq \frac{2\delta_f}{m\theta(1-\epsilon_v)}\,,\ ||e_{\tilde{R}}|| \leq \frac{2-c^2}{2}\frac{\delta_\omega}{\theta} \tag{39}$$
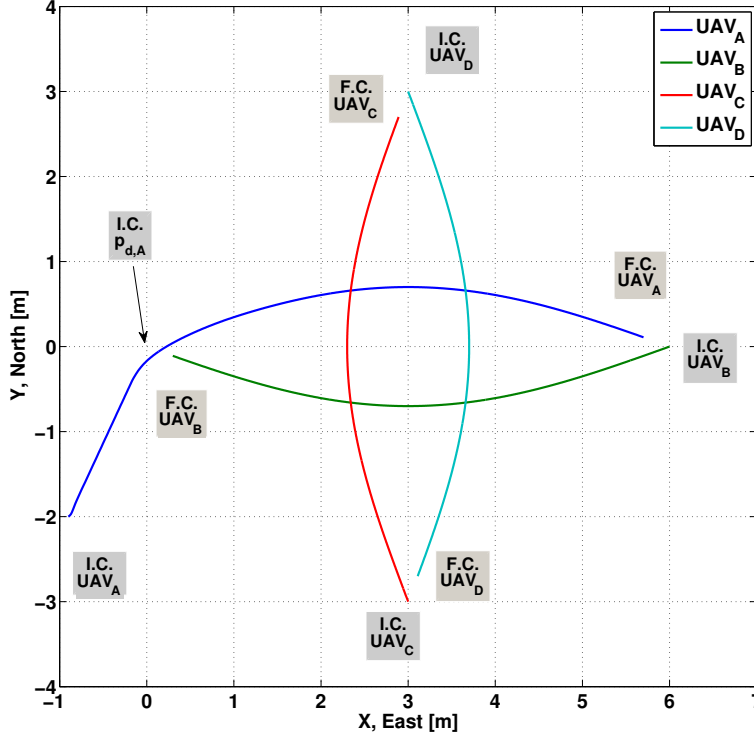

Fig. 3: Symmetric exchange of position of four Quadrotors with initial PF error (UAV_A)

[10] S. L. Waslander, G. M. Hoffman, J. S. Jang, and C. J. Tomlin, "Multi-agent quadrotor testbed control design: integral sliding mode vs reinforcement learning," in *International Conference on Intelligent Robots and Systems*, 2005, pp. 468–473.

[11] T. Lee, M. Leok, and N. H. McClamroch, "Control of complex maneuvers for a quadrotor UAV using geometric methods on SE(3)," *IEEE Transactions on Automatic Control*, 2010, submitted. Available online: arXiv:1003.2005v3.

[12] V. Cichella, I. Kaminer, V. Dobrokhodov, E. Xargay, N. Hovakimyan, and A. Pascoal, "Geometric 3d path-following control for a fixed-wing uav on SO(3)," in *AIAA Guidance, Navigation and Control Conference*, Portland, Oregon, August 2011, AIAA-2011-6415.

[13] E. Xargay, I. Kaminer, A. M. Pascoal, N. Hovakimyan, V. Dobrokhodov, V. Cichella, A. P. Aguiar, and R. Ghabcheloo, "Time-critical cooperative path following of multiple UAVs over time-varying networks," submitted to *IEEE Transactions on Control System Thechnology*, 2011.

[14] M. Mesbahi and F. Y. Hadaegh, "Formation flying control of multiple spacecraft via graphs, matrix inequalities, and switching," *Journal of Guidance, Control and Dynamics*, vol. 24, no. 2, pp. 369–377, March–April 2001.

[15] Y. D. Song, Y. Li, and X. H. Liao, "Orthogonal transformation based robust adaptive close formation control of multi-UAVs," in *American Control Conference*, vol. 5, Portland, OR, June 2005, pp. 2983–2988.

[16] D. M. Stipanović, G. İnalhan, R. Teo, and C. J. Tomlin, "Decentralized overlapping control of a formation of unmanned aerial vehicles," *Automatica*, vol. 40, no. 8, pp. 1285–1296, August 2004.

[17] R. Ghabcheloo, A. M. Pascoal, C. Silvestre, and I. Kaminer, "Coordinated path following control of multiple wheeled robots using linearization techniques," *International Journal of Systems Science*, vol. 37, no. 6, pp. 399–414, May 2006.

[18] R. Ghabcheloo, A. P. Aguiar, A. M. Pascoal, C. Silvestre, I. Kaminer, and J. P. Hespanha, "Coordinated path-following control of multiple underactuated autonomous vehicles in presence of communication failures," in *IEEE Conference on Decision and Control*, San Diego, CA, December 2006, pp. 4345–4350.

[19] F. L. Pereira and J. B. de Sousa, "Coordinated control of networked vehicles: An autonomous underwater system," *Automation and Remote Control*, vol. 65, no. 7, pp. 1037–1045, July 2004.

[20] I. Kaminer, A. M. Pascoal, E. Hallberg, and C. Silvestreo, "Trajectory tracking for autonomous vehicles: An integrated approach to guidance and control," *Journal of Guidance, Control and Dynamics*, vol. 21, no. 1, pp. 29–38, January–February 1998.

[21] Y. Kim and M. Mesbahi, "On maximizing the second smallest eigenvalue of state-dependent graph Laplacian," *IEEE Transactions on Automatic*
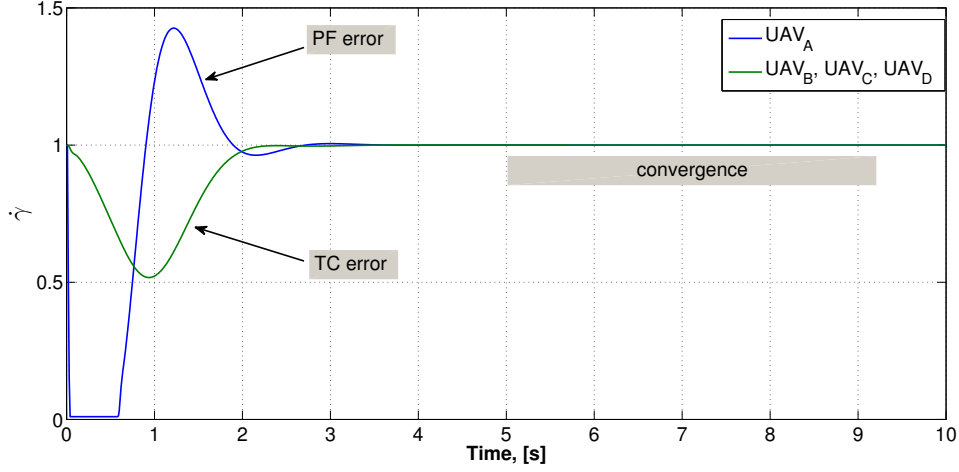
Fig. 4: $\dot{\gamma}_A$, $\dot{\gamma}_B$, $\dot{\gamma}_C$ and $\dot{\gamma}_D$ converge to 1
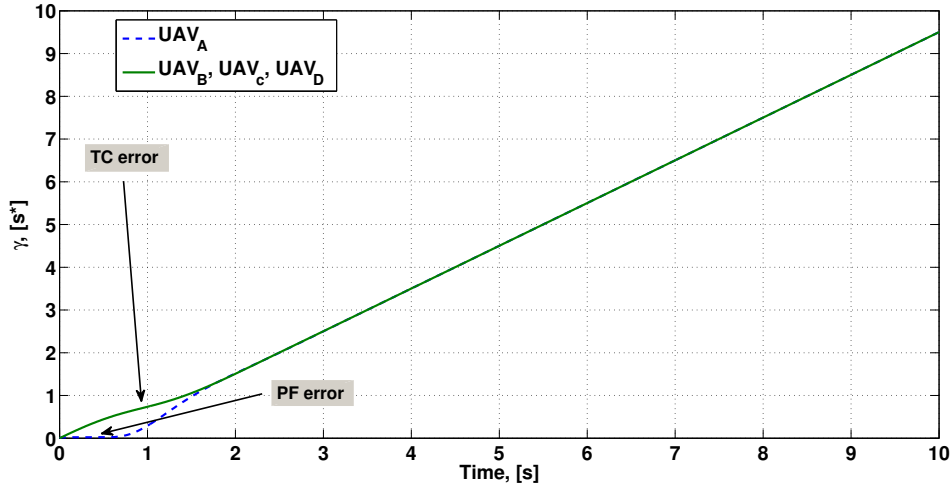

Fig. 5: *Virtual time γ_A, γ_B, γ_C and γ_D converge to the same value*

Control, vol. 51, no. 1, pp. 116–120, January 2006.

[22] T. Lee, "Robust adaptive geometric tracking controls on so(3) with an application to the attitude dynamicsof a quadrotor uav," 2011, available: http://arxiv.org/abs/1108.6031.

[23] N. Biggs, *Algebraic Graph Theory*. New York, NY: Cambridge University Press, 1993.

[24] A. Loría and E. Panteley, "Uniform exponential stability of linear time-varying systems: Revisited," *Systems & Control Letters*, vol. 47, no. 1, pp. 13–24, September 2002.

[25] H. K. Khalil, *Nonlinear Systems*. Englewood Cliffs, NJ: Prentice Hall, 2002.

APPENDIX

A. *Outline of the proof of Lemma 1*

To prove the exponential convergence of the TCPF error vector defined in (30), first note that the following system

$$\dot{\phi}(t) = -\bar{L}\phi(t)$$

is GUES [24], with $\bar{L}$ satisfying the PE assumption in (19).

Furthermore, choosing the following transformation operator

$$\chi(t) = b\xi(t) + Qz(t)$$

the dynamic of the TC error can be written as

$$\begin{cases} \dot{\chi} = -\frac{a}{b}\bar{L}\chi + \frac{a}{b}QLz - Q\bar{\alpha}(e_x, e_v) \\ \dot{z} = -(bI - \frac{a}{b}L)z - \frac{a}{b}LQ^\top\chi - \bar{\alpha}(e_x, e_v). \end{cases}$$

Therefore, leveraging the approach in [11] for V_{PF} by adding two extra terms representing the TC problem (V_{TC}), the function

$$V = \underbrace{\frac{k_x}{2}||e_x||^2 + \frac{m}{2}||e_v||^2 + \Psi(\tilde{R}) + c_1(e_v^\top e_x)}_{V_{PF}} + \underbrace{\chi^\top P_c\chi + \frac{1}{2}||z||^2}_{V_{TC}}, \tag{40}$$

where k_x, m, c_1 were introduced in Section II and Lemma 1, and P_c is discussed in details in [25, Theorem 4.12], can be chosen as a new
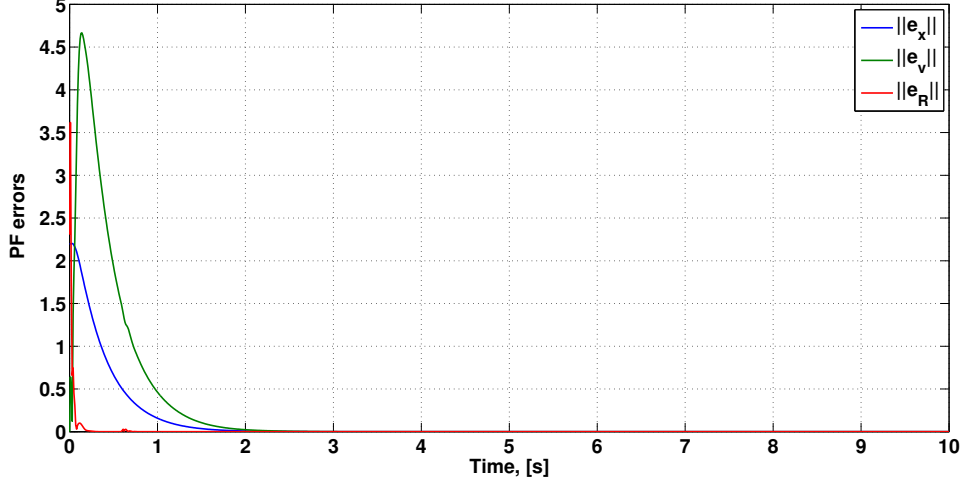
Fig. 6: UAV$_A$: PF errors $||e_x||$, $||e_v||$ and $||e_{\tilde{R}}||$ converge to zero

Lyapunov candidate function. Then, following the same arguments used in [24, Lemma 2] and [11], the following bound holds:

$$
\begin{aligned}
\dot{V} =& \dot{V}_{PF} + \dot{V}_{TC} \\
\leq& -\frac{c_1 k_x}{m}(1-c^2)||e_x||^2 - (k_v(1-c^2) - c_1)||e_v||^2 + \\
& - k_{\tilde{R}}||e_{\tilde{R}}||^2 + \frac{c_1 k_v}{m}(1+c^2)||e_x||||e_v|| + \\
& + (k_x e_{x\,\max\,i} + B)||e_{\tilde{R}}||||e_v|| + \frac{B_i c_1}{m}||e_{\tilde{R}}||||e_x|| + \\
& + (k_x b_1 + c_1 b_2)||z||||e_x|| + (c_1 b_1 + m b_2)||z||||e_v|| + \\
& - \bar{c}_3||\chi||^2 - (b-n)||z||^2 + n\left(\frac{\bar{c}_4}{\gamma_\lambda} + 1\right)||\chi||||z||.
\end{aligned}
\tag{41}
$$

Finally, it can be proven that there exist k_x, k_v, $k_{\tilde{R}}$, c_1, a and b such that

$$
\dot{V} \leq -\lambda V
\tag{42}
$$

with domain of attraction defined in (34), and rate of convergence λ defined in (31). therefore leading to the following:

$$
V(t) \leq V(0)e^{-\lambda t}.
$$

Thus, the result of Lemma 1 immediately follows.

B. *Outline of the proof of Lemma 2*

Start by considering the Lyapunov function in (40). Following the same outline described in Appendix A, and after some algebraic manipulations (the reader is referred to [13, Appendix C]) we get:

$$
\begin{aligned}
\dot{V} =& \dot{V}_{PF} + \dot{V}_{TC} \\
\leq& -\frac{c_1 k_x}{m}(1-c^2)||e_x||^2 - (k_v(1-c^2) - c_1)||e_v||^2 + \\
& - k_{\tilde{R}}||e_{\tilde{R}}||^2 + \frac{c_1 k_v}{m}(1+c^2)||e_x||||e_v|| + \\
& + (k_x e_{x\,\max\,i} + B)||e_{\tilde{R}}||||e_v|| + \frac{B_i c_1}{m}||e_{\tilde{R}}||||e_x|| + \\
& + (k_x b_1 + c_1 b_2)||z||||e_x|| + (c_1 b_1 + m b_2)||z||||e_v|| + \\
& - \bar{c}_3||\chi||^2 - (b-n)||z||^2 + n\left(\frac{\bar{c}_4}{\gamma_\lambda} + 1\right)||\chi||||z|| \\
& + \frac{c_1}{m}\delta_f||e_x|| + \delta_f||e_v|| + \frac{1}{2}\delta_\omega||e_{\tilde{R}}||.
\end{aligned}
\tag{43}
$$

Recalling the result in (42), and following a proof in [25, Lemma 9.2], leads to

$$
\begin{aligned}
\dot{V} \leq& -(\lambda - \theta)V - \theta\left(\frac{k_x}{2}||e_x||^2 + \frac{m}{2}||e_v||^2 + \frac{1}{2-c^2}||e_{\tilde{R}}||^2 + \right. \\
& \left. + c_1(e_v^\top e_x) + \chi^\top P_c \chi + \frac{1}{2}||z||^2\right) + \\
& + \frac{c_1}{m}\delta_f||e_x|| + \delta_f||e_v|| + \frac{1}{2}\delta_\omega||e_{\tilde{R}}||,
\end{aligned}
$$

where $0 < \theta < \lambda$.

Therefore, after straightforward computations, we can show that outside the bounded set

$$
\begin{aligned}
\Omega_d \triangleq& \left\{ x = [e_x^\top, e_v^\top, e_{\tilde{R}}^\top, \chi^\top, z^\top]^\top \text{ s.t.} \right. \\
& ||e_x|| \leq \frac{2c_1\delta_f}{k_x m\theta(1-\epsilon_x)}, ||e_v|| \leq \frac{2\delta_f}{m\theta(1-\epsilon_v)}, \\
& \left. ||e_{\tilde{R}}|| \leq \frac{2-c^2}{2}\frac{\delta_\omega}{\theta} \right\},
\end{aligned}
$$

the following bound holds:

$$
\dot{V} \leq -(\lambda - \theta)V.
$$

Finally, letting γ_p, γ_q, γ_r and γ_f satisfy the bounds in (36) and (37) implies that $\Omega_d \subset \Omega_c$, thus proving Lemma 2.